engineering proceedings

MDPI

Proceeding Paper

First Test of a Multi-Constellation, Multi-Frequency GNSS Receiver on Board a Sounding Rocket †

Benjamin Braun [1,*], Markus Markgraf [1], Lennart Rheinwald [1], Sebastian Weiß [2] and Marcus Hörschgen-Eggers [2]

[1] German Space Operations Center (GSOC), German Aerospace Center (DLR), Münchener Str. 20, D-82334 Weßling, Germany; markus.markgraf@dlr.de (M.M.); lennart.rheinwald@dlr.de (L.R.)
[2] Mobile Rocket Base (MORABA), German Aerospace Center (DLR), Münchener Str. 20, D-82334 Weßling, Germany; se.weiss@dlr.de (S.W.); marcus.hoerschgen-eggers@dlr.de (M.H.-E.)
* Correspondence: benjamin.braun@dlr.de
† Presented at the European Navigation Conference 2025 (ENC 2025), Wrocław, Poland, 21–23 May 2025.

Abstract

The paper shows the results of a first test of two multi-constellation, multi-frequency GNSS receivers on board the MAPHEUS-15 sounding rocket, which was launched from Esrange, Sweden, on 11 November 2024. During the flight, the GNSS receivers tracked the signals from up to 37 satellites simultaneously and were thus able to continuously compute a navigation solution from lift-off until atmospheric reentry and during the landing phase on the parachute, even in the presence of jamming. The flight test showed that the robustness of the navigation solution could be noticeably improved by increasing the number of constellations and signals.

Keywords: GNSS; multi-constellation; multi-frequency; sounding rocket; MORABA; Esrange; jamming; interference; power spectral density; Scandinavia

1. Introduction

DLR's Mobile Rocket Base (MORABA) traditionally uses GNSS to determine the trajectories of their sounding rockets. Accurate trajectories are required, for example, for range safety purposes, flight performance analyses or data fusion with inertial measurements to estimate orientation. Until 2024, MORABA's sounding rocket vehicles were equipped with L1-only GNSS receivers, such as the long-serving DLR developed Phoenix GPS receiver or the NovAtel OEM719 receiver [1].

Since 2022, the GNSS receivers on board the sounding rockets launched from northern Scandinavia have experienced jamming on the L1 frequency in a way that reliable computation of a navigation solution was impossible above altitudes of around 25 km [2]. This fact motivated the test of GNSS receivers that can also receive other signals in the L-band in addition to L1 from all available navigation satellite constellations.

On 11 November 2024, 07:38 (UTC), MORABA launched the MAPHEUS-15 sounding rocket from Esrange, which reached an apogee altitude of 309 km, and whose flight trajectory is shown in Figure 1 [3,4]. In addition to a NovAtel OEM719 GPS+Galileo L1 GNSS receiver, which is an integral part of the service module of the MAPHEUS sounding rocket, two multi-constellation, multi-frequency GNSS receivers, a Septentrio AsteRx-m3 Pro+ and a Septentrio mosaic-X5, were installed on board. The receivers tracked GPS L1 C/A, L2C and L5 signals, Galileo E1, E5a, E5b and E5 signals, BeiDou B1I, B3I, B1C and B2a signals and GLONASS L1 C/A, L2 C/A and L3OC signals.

Academic Editor: Tomasz Hadaś

Published: 13 March 2026

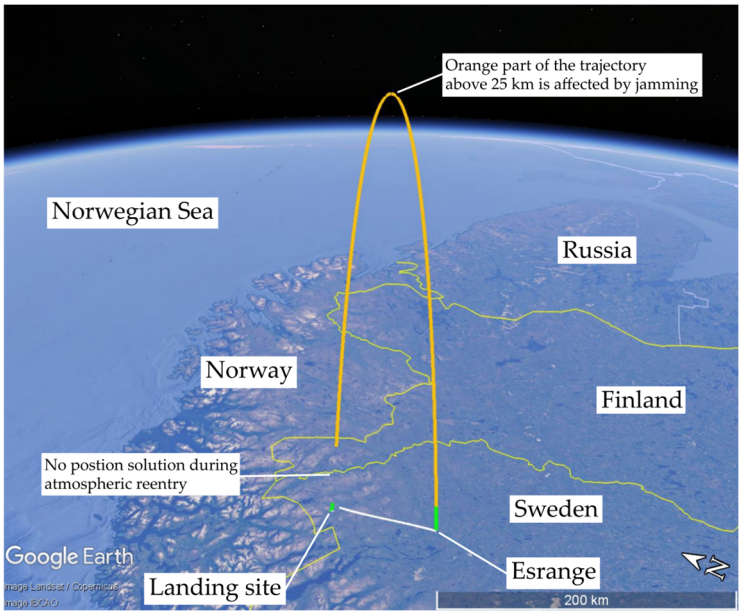

Figure 1. Trajectory of the MAPHEUS-15 sounding rocket. During the ascent and descent, no interference was observed at altitudes below 25 km (green sections of the flight trajectory). Above 25 km, the reception of GNSS signals was interfered (orange section of the flight trajectory).

To receive signals with frequencies in the range between 1164 and 1610 MHz, new multi-frequency GNSS antennas were developed for nose tip and side mounting. The potential of using multi-constellation becomes obvious by the sky plot in Figure 2.

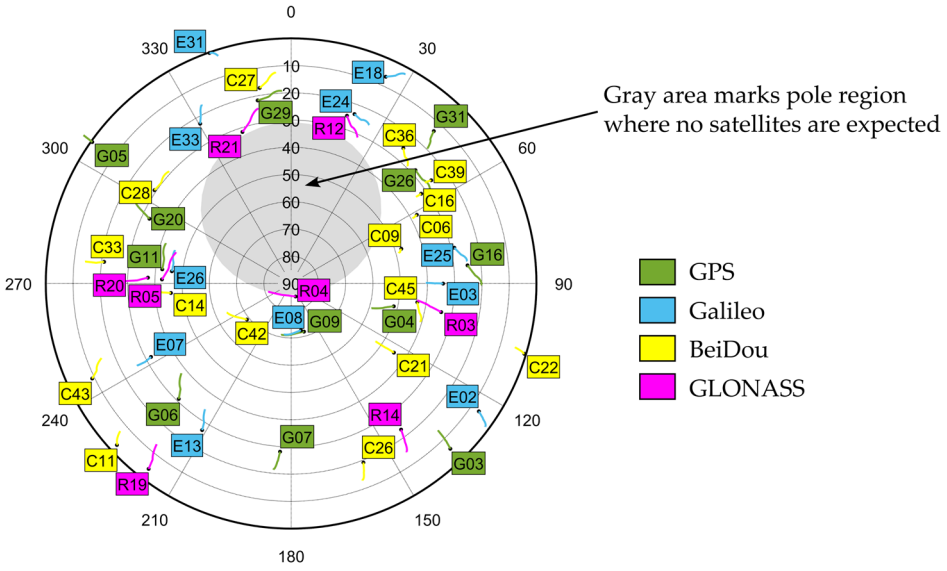

Figure 2. Sky plot along the trajectory of MAPHEUS-15 w.r.t. the local horizontal plane.

2. Challenges of Using GNSS on Sounding Rockets

The use of GNSS on sounding rockets faces numerous challenges from lift-off, propelled ascent, coasting, atmospheric re-entry, to parachute landing.

Esrange features a launch tower which covers the launch pad and rail and protects the sounding rocket from precipitation and very cold temperatures in winter during the preparation and checkout phases before lift-off, as shown in Figure 3. As the walls of the launch tower are not radio transparent, a GNSS reradiation kit was installed inside the launch tower to relay GNSS signals so that the GNSS receivers on board the sounding rocket are able to acquire and track GNSS signals before lift-off.

https://doi.org/10.3390/engproc2026126039

Figure 3. Launch tower (**left**) and MAPHEUS-15 leaving the launch tower (**right**) (Credit: SSC).

Shortly after lift-off, the sounding rocket passes the tube at the top of the launch tower, as shown on the right in Figure 3. During this very brief moment, the GNSS receivers receive neither the GNSS signals from the reradiation kit inside nor the real signals outside the tower and consequently lose tracking of all signals. Outside the tower, the velocity of the sounding rocket is already very high due to the high initial acceleration, which makes it difficult to quickly reacquire the lost signals. In addition, the strengths of the real signals outside differ significantly from those reradiated inside the tower.

Immediately afterwards, the sounding rocket is spun up to a roll rate of up to 2000 deg/s to reduce the deviation from the nominal flight path during the propelled flight phase. This roll rate is only stopped again outside the dense part of the atmosphere after motor burnout. Special antennas are required for the continuous reception of GNSS signals during this phase, such as wraparound antennas or individual antenna elements distributed around the circumference of the rocket body, whose signals are combined. The nose tip, which is an ideal location for a GNSS antenna, is unfortunately not always available, as the nose cone is often jettisoned during flight, e.g., to expose scientific experiments on the payload's forefront to the outside world or to be able to deploy the drogue and main parachutes by the flight recovery system. The measurements of the GNSS receiver are affected by the phase wind-up effect, and high vibration acts on the local oscillator of the GNSS receiver during the propelled flight phase increasing the measurement noise.

As explained in detail in [1], sounding rockets launched from Esrange have been increasingly exposed to jamming above an altitude of around 25 km since 2022. This interference, mainly in the L1 frequency range, reduces the carrier-to-noise ratio of the tracked signals and can lead to the loss of the tracked signals. As shown in [5–7], for example, this type of large-scale jamming can even be observed on satellites in low Earth orbit (LEO). Later, during atmospheric reentry below an altitude of about 60 km, the payload rapidly slews around due to large aerodynamic forces and moments which is again challenging for continuous signal tracking. Only after the parachutes have been deployed, conditions get better again.

3. Test Setup

3.1. GNSS Antenna and Receiver Hardware

The payload of the MAPHEUS-15 sounding rocket is shown in Figure 4. It is equipped with several GNSS antennas: a multi-frequency antenna prominently located at the nose tip, four L1 blade antennas tuned to signal frequencies around 1575 MHz and mounted at 90 degrees around the circumference of the payload, and two L2/L5 blade antennas tuned to signal frequencies around 1200 MHz and mounted on opposite sides of the payload. MAPHEUS-15's nose cone is jettisoned right at the apogee of the flight trajectory, so that the

nose tip antenna is used during the ascent and the blade antennas during the descent. The internal setup of the GNSS components is illustrated in Figure 5. The green components are part of the standard service module and have been used before, the yellow components were added for the multi-constellation, multi-frequency GNSS receiver test. The signals of the four L1 blade antennas and the two L2/L5 blade antennas are each superimposed in signal combiners. R/F relays are used to select either the signals from the nose tip antenna or the combined signals from the blade antennas.

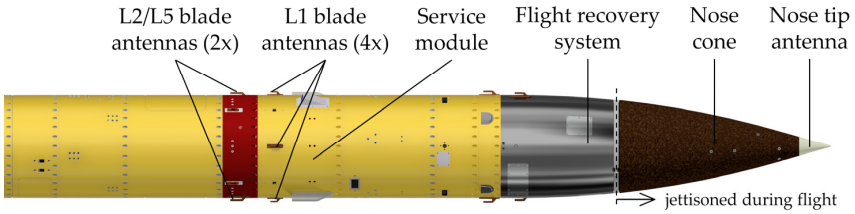

Figure 4. MAPHEUS-15 payload showing the service module, the flight recovery system, the nose cone, and the mounting locations of the GNSS antennas.

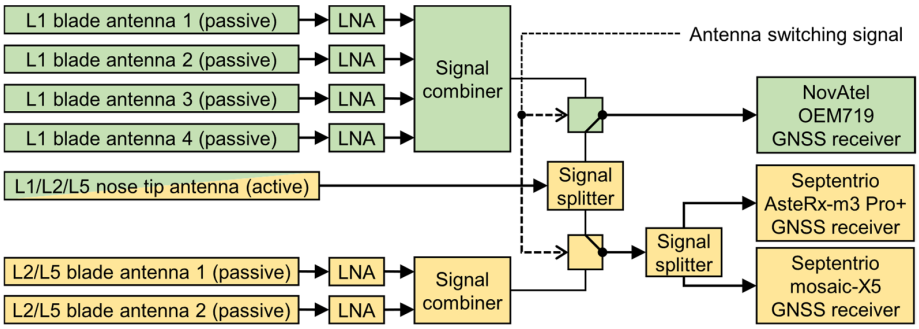

Figure 5. Setup of the GNSS components. The green colored components belong to the service module, the yellow ones are part of the multi-constellation, multi-frequency GNSS receiver test.

3.2. Antenna Development

The previously used nose tip antenna was a single-frequency antenna that only received signals in the L1 frequency band. A new nose tip antenna was developed in order to also be able to use the signals in the L2 and L5 frequency bands. The antenna is based on MAXTENA's M9PLUS-HCT-A-EMB active embedded multi-frequency antenna element, which is integrated into a nose-tip structure made of PEEK material to withstand the high temperatures during ascent and descent in the dense atmosphere.

The L1 blade antennas used to date are tuned to frequencies around 1575 MHz. A new blade antenna element had been developed that is tuned to frequencies around 1200 MHz so that it receives signals in the L2 and L5 bands. Even though the design of the blade antennas is naturally not optimal for the reception of circularly polarized GNSS signals, it has only a minor aerodynamic influence and is robust and stable against high temperatures thanks to the use of copper material. As the blade antennas are passive, a new low-noise amplifier (LNA) was also developed for signals in the L2 and L5 bands.

The performance of the new nose tip antenna and the new L2/L5 blade antenna was tested and characterized with a static roof antenna test campaign prior to the MAPHEUS-15 flight. These tests showed that the L2/L5 blade antenna can also receive signals in the L1 frequency band, although the signal strength is around 6 dB lower.

3.3. Receiver Configuration

The Septentrio AsteRx-m3 Pro+ and Septentrio mosaic-X5 GNSS receivers selected for the multi-constellation, multi-frequency GNSS receiver test are commercial-off-the-shelf

receivers that are not designed per se for use on highly dynamic vehicles such as sounding rockets. In particular, the unique conditions during lift-off with high acceleration and jerk and the short interruption of signals in the launch tower tube require highly dynamic tracking loops that are able to quickly reacquire and track lost signals after leaving the launch tower. The GNSS receivers offer the possibility to tune the bandwidths of the delay lock loop (DLL) and the phase lock loop (PLL), and the signal integration time. The parameters can be fixed or adaptive, so that the receiver automatically adjusts the parameters of the tracking loop to the current dynamics. With numerous tests with a GNSS signal simulator in the laboratory prior to the MAPHEUS-15 flight, optimal settings in terms of reacquisition time and deviation of the position solution from the nominal trajectory were identified for the GPS L1 C/A and L5 and Galileo signals. Adaptation was explicitly switched off for these signals. For all other signals, the default settings were not changed. The selected tracking loop parameters are listed in Table 1.

Table 1. Configuration of the tracking loop parameters. Non-default values that were set manually for the flight test are printed in bold. All other values correspond to the default factory settings of the Septentrio GNSS receiver.

Signals	Single-Sided Tracking Loop Bandwidth [Hz]		(Maximum) Integration Time [ms]		Adaptive?
	DLL	PLL	DLL	PLL	
GPS L1 C/A, L5	**0.10**	**17**	100	**1**	**no**
GPS L2C	0.25	15	100	10	yes
Galileo E1, E5	**0.10**	**17**	100	**2**	**no**
all other signals	0.25	15	100	10	yes

4. Flight Results

The Septentrio AsteRx-m3 Pro+ and mosaic-X5 GNSS receivers showed comparable performance. The following discussion therefore refers exclusively to the flight results of the mosaic-X5 GNSS receiver. The NovAtel OEM719 L1-only GPS+Galileo GNSS receiver did not reacquire and track GPS or Galileo signals after leaving the launch tower and is not considered in the following. Figure 6 illustrates the number of tracked GPS, Galileo, BeiDou and GLONASS satellites, and the altitude computed from the GNSS measurements. The vertical dashed lines indicate the altitude of 25 km during the ascent at T + 26.5 s and the switching from the multi-frequency nose tip antenna to the L2/L5 blade antennas at apogee at T + 275 s. The GNSS receiver is able to continuously calculate a position solution, except between T + 0 s and T + 4.5 s at altitudes below 1.1 km when MAPHEUS-15 leaves the launch tower, and between T + 507.5 s and T + 584.9 s at altitudes between 66 km and 8.9 km during the atmospheric reentry.

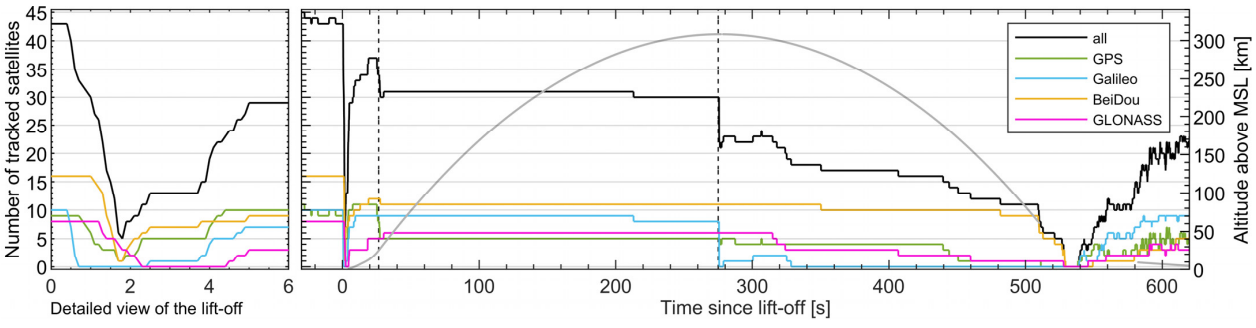

Figure 6. Number of tracked satellites. The vertical dashed line at T + 26.5 s marks the beginning of the jamming and at T + 275 s the switching from the nose tip antenna to the blade antennas.

Figure 7 shows the tracking status of all GPS, Galileo and BeiDou signals. The GPS IIR satellites only transmit L1 C/A signals, the GPS IIR-M satellites transmit L1 C/A and L2C signals and the GPS IIF and GPS IIIA satellites transmit all signals. The BeiDou-2 satellites only broadcast B1I and B3I signals, the BeiDou-3 satellites broadcast all signals.

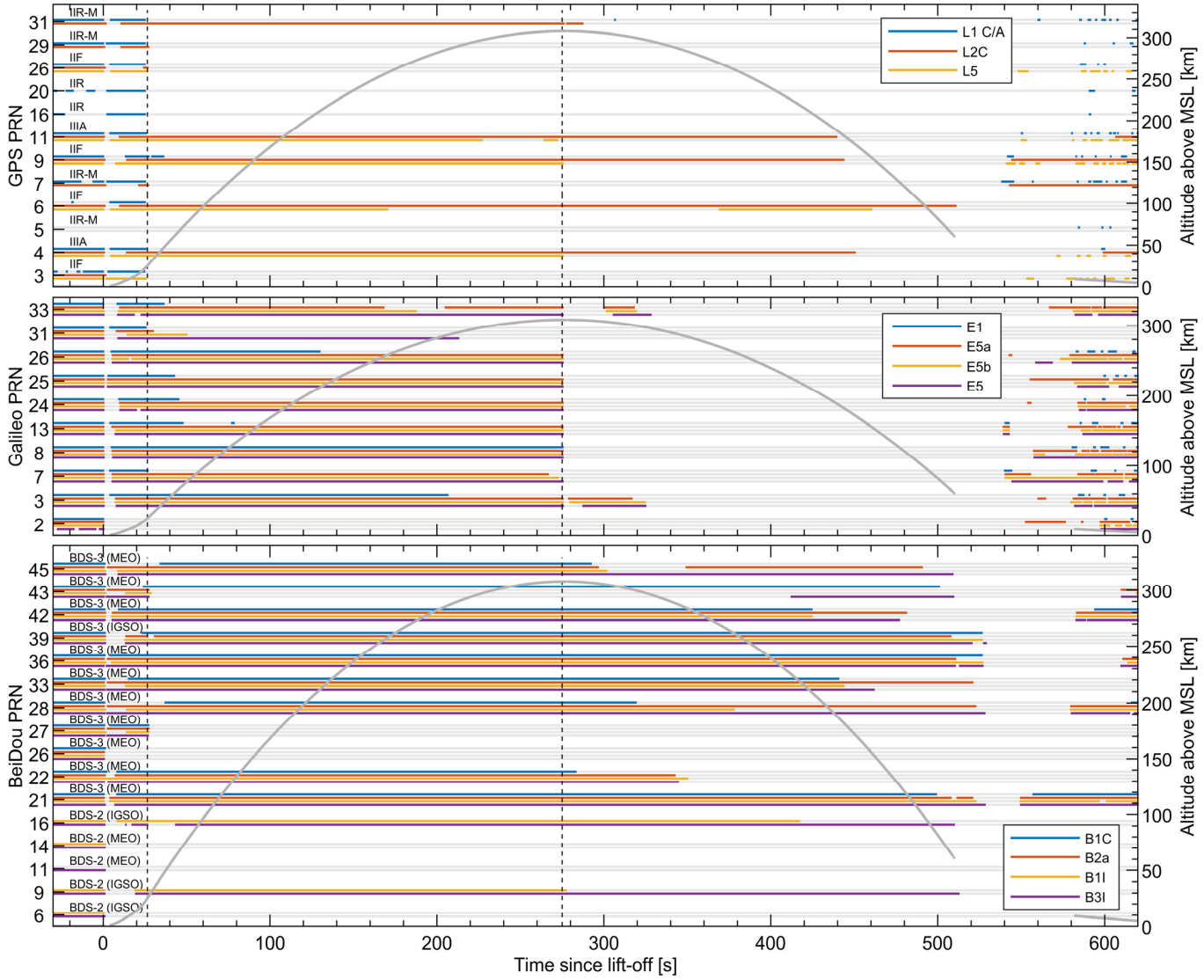

Figure 7. Tracked GPS, Galileo and BeiDou signals. Tracked GLONASS signals are not shown.

As expected, the GNSS receiver loses tracking of almost all signals shortly after lift-off except for single signals from one GPS and one BeiDou satellite, but successively regains tracking. While the recovery of the GPS L1 C/A and L5 signals is quite fast, it takes a little longer for the GPS L2C signals. The reacquisition of Galileo signals generally seems to take a little longer, but all signals are reacquired more or less simultaneously. The reacquisition of signals from the BeiDou-3 satellites is faster than of signals from the older BeiDou-2 satellites and works fairly fast for the BeiDou-3 satellites.

At an altitude of around 25 km, when jamming begins to interfere with signal reception, tracking of the GPS L1 C/A signals is lost immediately. Tracking of L2C and L5 signals is less affected and is only lost for some satellites. However, L5 signals are gradually lost during ascent, whereas the tracking of L2C signals appears to be more robust. Tracking of Galileo signals is generally less affected, but Galileo E1 signals are also successively lost during the ascent and signals in the E5 band are tracked more robustly. The BeiDou signals are hardly affected by the interference.

At T + 275 s, when switching from the helical multi-frequency nose tip antenna to the L2/L5 blade antennas, the remaining GPS L5 signals are finally lost, and the tracking of almost all Galileo signals ends abruptly. Interestingly, solely the BeiDou signals do not appear to be influenced by the antenna switching. The signal loss can be explained by the signal quality provided by the two antennas: while the circularly polarized nose tip antenna features an almost optimal, hemispherical reception pattern, the two combined blade antennas receive less signal power due to their linear polarization and have a much more inhomogeneous reception pattern. Tracking deteriorates due to the sudden drop in signal quality. With the beginning of the atmospheric reentry during the descent at an altitude of around 60 km, the payload starts to tumble very quickly, and the blade antennas with the inhomogeneous reception pattern no longer receive signals continuously. As a result, the GNSS receiver loses tracking of all signals and can no longer calculate a navigation solution. The situation only improves again when the rotation of the payload stabilizes, the descent velocity decreases and the payload falls below an altitude of around 25 km. Gradually, signal tracking is regained, and at an altitude of around 9 km, the GNSS receiver again outputs a valid navigation solution.

The above statements are emphasized by a look at the carrier-to-noise ratios (C/N_0 values) of the received signals in Figure 8. First of all, the C/N_0 values of all received signals outside the launch tower during the flight are generally below 45 dB-Hz and are therefore inherently quite low, which is mainly due to the small size of the antennas. However, the values are consistent with the values observed during the static roof antenna campaign. The C/N_0 values of the signals in the L1 band suddenly drop by around 5 dB when reaching the altitude of around 25 km during the ascent and further decrease by 4–5 dB in the sequel. The signals in the L2- and L5 bands drop by 3–5 dB, but in general do not further decrease afterwards. When switching the antennas at T + 275 s, the C/N_0 values of all signals decrease again. The C/N_0 values oscillate more excessively during the descent with the blade antennas than during the ascent with the nose tip antenna, which is due to a small angular motion of the payload and the more inhomogeneous reception pattern of the combined blade antennas. Only at low altitudes when signal tracking is regained after the atmospheric reentry, the levels of the C/N_0 values of all signals rise again to the values that were achieved directly after lift-off. In this flight phase, the C/N_0 values appear to be very noise which is because of the high angular rate of the payload in this phase.

It turns out that the tracking loops of the GPS L2C and BeiDou signals, whose DLL and PLL bandwidths and integration times were not changed and for which the adaptive steering was not deactivated, are more sensitive than the tracking loops of the GPS L1 C/A, L5 and Galileo signals with fixed bandwidths and integration times and deactivated adaptive steering (marked gray in Figure 8). GPS L2C and BeiDou signals are tracked down to 18 dB-Hz, while the other signals are only tracked down to 28 dB-Hz.

The reception of all signals seems to be affected by jamming at flight altitudes above around 25 km. To further substantiate this thesis, the spectrogram of the signal power in the L1 band is exemplarily shown in Figure 9. It is calculated from several millisecond-long snippets of digitized I/Q raw samples provided by the GNSS receiver. As with the flight data shown in [1], additional signal power with a bandwidth of 1–2 MHz is superimposed on the frequencies 1561.10 MHz and 1575.42 MHz (sharp yellow-red stripe) and broadband signal power is superimposed on the GLONASS L1 FDMA frequency range 1598.06–1605.38 MHz (broad light green stripe). Furthermore, additional, albeit lower, signal power can be recognized on the BeiDou B1I frequency 1561.10 MHz. Jamming is perceptible at all flight altitudes, even at the apogee of 309 km. The spectrograms of the L2 and L5 bands are not shown here. In contrast to the L1 band, no jamming signal power is visible on the dedicated navigation signal frequencies in the L2 and L5 bands. The power

of the jamming in the L2 and L5 bands, which appears to be present due to the decreasing C/N_0 values, is either lower than the noise floor or is time multiplexed and not covered by the I/Q sample snippets. The spectra of these two bands are in general unclean, because the bands are not reserved exclusively for GNSS. In the L5 band, e.g., short signal bursts appear from the distance measurement equipment of aircraft flying over northern Scandinavia. In addition, the noise floors are higher than in the L1 band and exhibit slow variations over the frequency range.

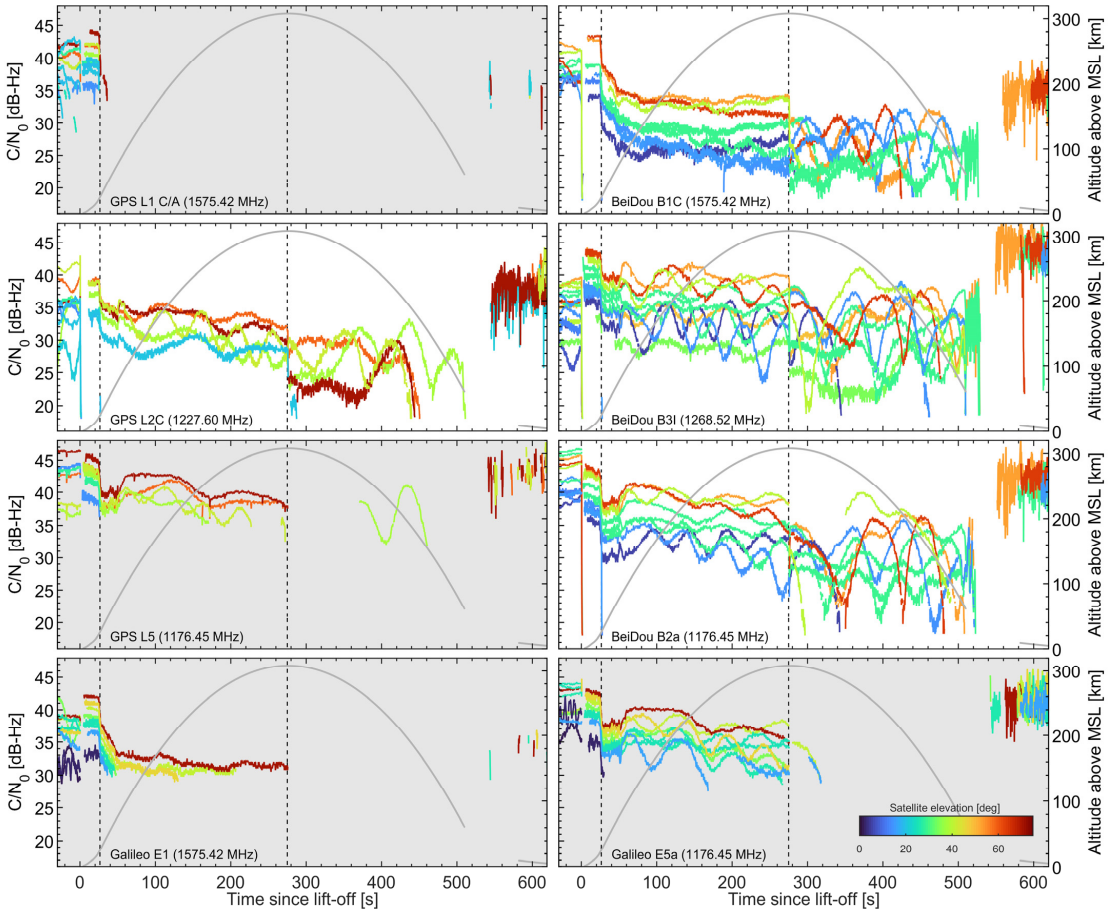

Figure 8. C/N_0 values of selected GPS, Galileo and BeiDou signals, with the line color representing the satellite's elevation. For the gray marked signals, adaptive tracking loops were deactivated.

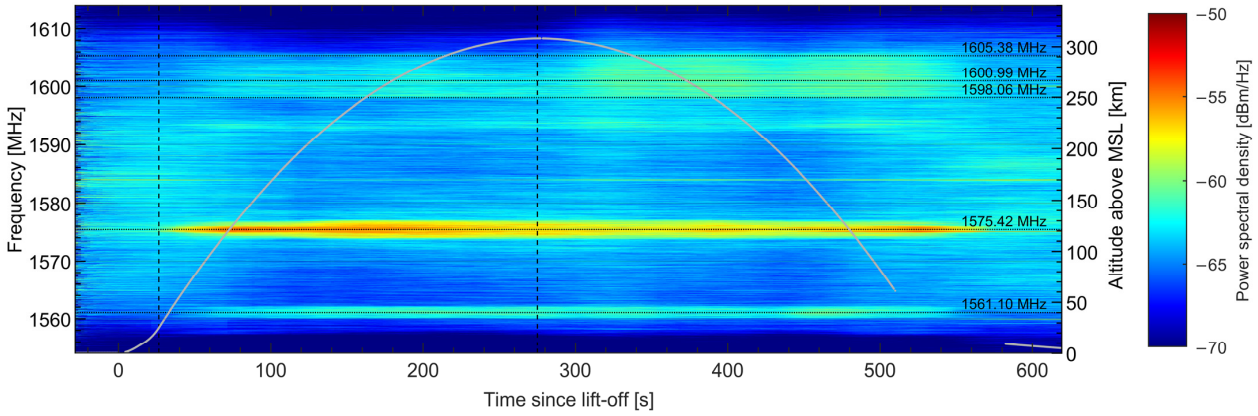

Figure 9. Signal power spectrogram of the L1 band.

https://doi.org/10.3390/engproc2026126039

5. Conclusions

During the flight, the GNSS receivers tracked the signals from up to 37 satellites simultaneously and were thus able to continuously compute a navigation solution from lift-off until atmospheric reentry, even in the presence of jamming. The flight test showed that the robustness of the navigation solution could be noticeably improved by increasing the number of constellations and signals. The adaptive tracking loop control enabled the tracking of very weak signals with a very low carrier-to-noise ratio down to 18 dB-Hz, so that the receivers were able to calculate position and velocity solutions almost during the entire flight, except for the atmospheric reentry phase. Tuning the tracking loop bandwidths and signal integration times did not yield a significant improvement. Further studies and tests need to be done to find the optimal tracking loop settings. The C/N_0 values suggest that all navigation signals in the L1, L2 and L5 bands are affected by jamming above an altitude of around 25 km up to apogee. However, looking at the signal power spectrograms, jamming signal power is only clearly visible in the L1 band but not directly in the L2 and L5 bands. Next, new multi-frequency patch antennas will be developed to replace the non-optimal blade antennas, which will be fully embedded in the payload structure. By arranging up to nine patch antenna elements around the circumference of the payload and cleverly combining the individual signals using phase delay elements, symmetrical and almost uniform antenna gain patterns can be generated compared to an antenna system consisting of just two opposing antenna elements [8].

Author Contributions: Conceptualization, B.B., M.M., L.R. and S.W.; experimentation, L.R., M.M. and S.W.; data post-processing, B.B. and S.W.; visualization, B.B.; writing—original draft preparation, B.B.; writing—review and editing, M.M., L.R., S.W. and M.H.-E.; project administration, M.H.-E. All authors have read and agreed to the published version of the manuscript.

Funding: This research received no external funding.

Institutional Review Board Statement: Not applicable.

Informed Consent Statement: Not applicable.

Data Availability Statement: The raw data supporting the conclusions of this article cannot be made available by the authors. This is due to legal restrictions imposed by the use of GNSS on sounding rockets flying faster than 600 m/s, amongst others.

Acknowledgments: The authors would like to thank the MORABA team for the accommodation of the GNSS receiver experiment on the MAPHEUS-15 sounding rocket on short notice and for their support during the campaigns.

Conflicts of Interest: The authors declare no conflict of interest.

References

1. Markgraf, M. The Phoenix GPS Receiver—A Practical Example of the Successful Application of a COTS-Based Navigation Sensor in Different Space Missions. In Proceedings of the 8th Annual IEEE International Conference on Wireless for Space and Extreme Environments (WISEE 2020), Vicenza, Italy, 12–14 October 2020.
2. Braun, B.; Montenbruck, O.; Markgraf, M.; Hörschgen-Eggers, M.; Kirchhartz, R. GNSS Jamming Observed on Sounding Rocket Flights from Northern Scandinavia. *Eng. Proc.* **2025**, *88*, 55. [CrossRef]
3. Weigand, A.C.; Berndl, M.; Kuhn, M.; Stadler, L.; Werneth, J.; Kirchhartz, R.; Kallenbach, A. Development and Qualification of the Solid Propellant Red Kite Sounding Rocket Motor. In Proceedings of the AIAA SCITECH 2026 Forum, Orlando, FL, USA, 12–16 January 2026. [CrossRef]
4. Scheuerpflug, F.; Röhr, T.H.; Huber, T.; Hargarten, D.A.; Kirchhartz, R.; Kuhn, M.; Weigand, A.; Berndl, M.; Werneth, J. Red Kite Sounding Rocket Motor—Qualification and Application Spectrum. *J. Spacecr. Rocket.* **2025**, *62*. [CrossRef]
5. Murrian, M.J.; Narula, L.; Iannucci, P.A.; Budzien, S.; O'Hanlon, B.W.; Powell, S.P.; Humphreys, T.E. First results from three years of GNSS interference monitoring from low Earth orbit. *Navig. J. Inst. Navig.* **2021**, *68*, 673–685. [CrossRef]

6. Clements, Z.; Humphreys, T.E.; Ellis, P. Dual-Satellite Geolocation of Terrestrial GNSS Jammers from Low Earth Orbit. In Proceedings of the 2023 IEEE/ION Position, Location and Navigation Symposium (PLANS), Monterey, CA, USA, 24–27 April 2023; pp. 458–469. [CrossRef]
7. Menzione, F.; Picchi, O.M.; Senni, T.; Zelenevskiy, V.; Cucchi, L.; Piccolo, A.; Fortuny-Guasch, J. Interference Monitoring from Low Earth Orbit: The OPS-SAT Experiment. *Eng. Proc.* **2025**, *88*, 8. [CrossRef]
8. Klammsteiner, I.; Addo, E.O.; Tripathi, V.; Caizzone, S.A. Reconfigurable Analog Beamformer for Multi-Frequency, Multiantenna GNSS Applications. *Electronics* **2026**, *15*, 289. [CrossRef]

https://doi.org/10.3390/engproc2026126039